Diffraction by a right-angled impedance wedge

Andrey V. Osipov[1] and Thomas B. A. Senior[2]

Received 23 November 2007; revised 19 February 2008; accepted 6 March 2008; published 6 May 2008.

[1] A plane electromagnetic wave is incident at an oblique (skew) angle on a wedge of open angle $3\pi/2$ with scalar face impedances, the same on both faces. When the theory previously developed for wedges of arbitrary angle with tensor face impedances is specialized to this case, the analysis simplifies, and the resulting expressions for the geometrical optics, surface wave and diffracted fields are presented. Because of the practical importance of this geometry, a large set of figures is included showing the behavior of the diffracted field for a variety of face impedances.

Citation: Osipov, A. V., and T. B. A. Senior (2008), Diffraction by a right-angled impedance wedge, *Radio Sci.*, *43*, RS4S02, doi:10.1029/2007RS003787.

1. Introduction

[2] One of the most useful diffracting structures is a right-angled wedge of open angle $3\pi/2$ subject to impedance boundary conditions on the two faces. It is, for example, a key element in a physically-based model of wireless propagation in an urban environment when the wedge can represent the corner of a corridor in a building or of the building itself in a city street. For this purpose, however, we require a knowledge of the diffraction coefficient for a plane wave at oblique (skew) incidence on the wedge.

[3] For normal incidence the exact solution can be obtained using Maliuzhinets' technique [*Maliuzhinets*, 1958], but for skew incidence the exact solution was available only for specific values of the surface impedances [see, e.g., *Bernard*, 1998] or if one face of the wedge is perfectly conducting [*Vaccaro*, 1981; *Senior and Volakis*, 1986; *Rojas*, 1988]. Nevertheless, when neither face is perfectly conducting, a number of approximate solutions have been derived [*Syed and Volakis*, 1992; *Pelosi et al.*, 1998], and these are typically based on the assumption that the incidence is not far removed from normal. To solve the general scattering problem for impedance wedges, several approaches based on the reduction of the problem to integral equations [*Daniele and Lombardi*, 2006; *Lyalinov and Zhu*, 2006] and on the probabilistic random walk method [*Budaev and Bogy*, 2006] have been proposed in the past.

[4] Recently, a new method [*Osipov and Senior*, 2008] has been developed that provides the exact solution for a plane wave at any angle of incidence on an anisotropic impedance wedge of arbitrary angle. We now apply the method to a right-angled wedge having the same scalar impedance on both faces. Graphs showing the backscattered and bistatic scattering diffraction coefficients for a variety of surface impedances and incidence angles are presented. Furthermore, excitation of surface waves at the edge of the wedge is addressed analytically and numerically.

2. Formulation

[5] A wedge with open angle $3\pi/2$ is illuminated by an arbitrarily polarized plane electromagnetic wave having

$$\overline{E}_{\text{inc}} = \overline{E}_0 e^{i\overline{k}\cdot\overline{r}}, \quad \overline{H}_{\text{inc}} = \overline{H}_0 e^{i\overline{k}\cdot\overline{r}} \tag{1}$$

where a time factor $\exp(-i\omega t)$ has been assumed and suppressed. The wave is incident obliquely in the direction

$$\overline{k} = k(-\hat{x}\cos\phi_0 \sin\beta - \hat{y}\sin\phi_0 \sin\beta + \hat{z}\cos\beta) \tag{2}$$

where $\overline{r} = \hat{x}\rho\cos\phi + \hat{y}\rho\sin\phi + \hat{z}z$ is the position vector in a cylindrical coordinate system with z axis along the edge of the wedge, k is the wave number and $0 \le \phi_0 < 3\pi/4$, $0 < \beta < \pi$ (see Figure 1). The material properties of the wedge are represented by the impedance boundary condition

$$\hat{n} \times \overline{E} = Z_0 \eta \hat{n} \times \left(\hat{n} \times \overline{H}\right) \tag{3}$$

where η is the scalar impedance, the same on both faces, Z_0 is the free space impedance and $\hat{n} = \mp\hat{\phi}$ is the outward

[1]Microwaves and Radar Institute, German Aerospace Center, DLR, Wessling, Germany.
[2]Department of Electrical Engineering and Computer Science, University of Michigan, Ann Arbor, Michigan, USA.

0048-6604/08/2007RS003787

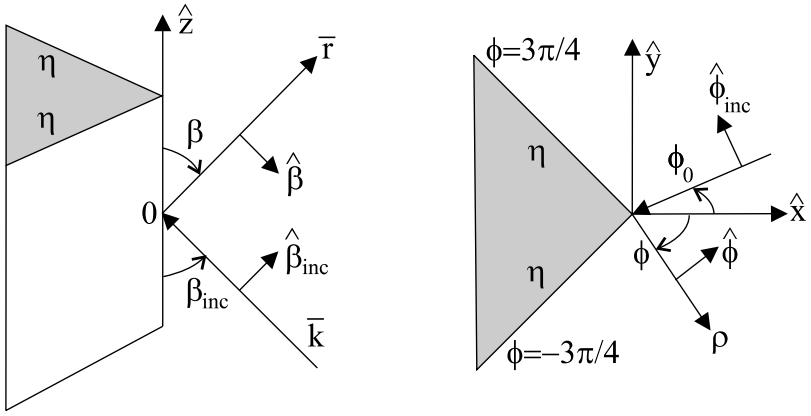

Figure 1. Wedge and the ray-fixed coordinate system.

unit vector normal to the wedge face $\phi = \pm 3\pi/4$. To ensure uniqueness it is assumed that Re $\eta > 0$.

[6] At the faces $\phi = \pm 3\pi/4$ the components of the boundary condition (3) are

$$E_\rho = \mp \eta Z_0 H_z, \quad E_z = \pm \eta Z_0 H_\rho \tag{4}$$

and since the total field must have the same z dependence as the incident field, these can be written as

$$\cos\beta \frac{\partial}{\partial \rho} E_z + \frac{1}{\rho}\frac{\partial}{\partial \phi}(Z_0 H_z) = \pm ik\eta \sin^2\beta Z_0 H_z \tag{5}$$

$$\frac{1}{\rho}\frac{\partial}{\partial \phi} E_z - \cos\beta \frac{\partial}{\partial \rho}(Z_0 H_z) = \pm \frac{ik}{\eta}\sin^2\beta E_z. \tag{6}$$

Following *Maliuzhinets* [1958], the total field components E_z and $Z_0 H_z$ are expressed as the Sommerfeld integrals

$$E_z(\rho,\phi,z) = \frac{e^{ikz\cos\beta}}{2\pi i}\int_\gamma e^{-ik\rho\sin\beta\cos\alpha} S_e(\alpha+\phi)d\alpha \tag{7}$$

$$Z_0 H_z(\rho,\phi,z) = \frac{e^{ikz\cos\beta}}{2\pi i}\int_\gamma e^{-ik\rho\sin\beta\cos\alpha} S_h(\alpha+\phi)d\alpha \tag{8}$$

where γ is the Sommerfeld double loop contour. The spectra $S_{e,h}(\alpha)$ must be such that

$$S_{e,h}(\alpha) = O(1), \quad |\mathrm{Im}\,\alpha| \to \infty \tag{9}$$

to ensure that $|E_z|, |H_z| = O(1)$ as $\rho \to 0$ (edge condition), and apart from a pole singularity at $\alpha = \phi_0$ with

$$\mathrm{res}\, S_e(\phi_0) = E_{0z}, \quad \mathrm{res}\, S_h(\phi_0) = Z_0 H_{0z} \tag{10}$$

which is necessary to recover the incident field (1), $S_{e,h}(\alpha)$ must be free of poles in the strip

$$\Pi_0 = \left\{\alpha : |\mathrm{Re}\,\alpha| \le \frac{3}{4}\pi\right\}. \tag{11}$$

[7] When (7) and (8) are inserted into (5) and (6), the boundary conditions demand

$$\overline{\overline{M}}_\pm(\alpha)\cdot\overline{S}\left(\alpha \pm \frac{3}{4}\pi\right) = \overline{\overline{M}}_\pm(-\alpha)\cdot\overline{S}\left(-\alpha \pm \frac{3}{4}\pi\right) \tag{12}$$

with

$$\overline{S}(\alpha) = \begin{bmatrix} S_e(\alpha) \\ \\ S_h(\alpha) \end{bmatrix} \tag{13}$$

and

$$\overline{\overline{M}}_\pm(\alpha) = \begin{bmatrix} M^\pm_{ee}(\alpha) & M^\pm_{eh}(\alpha) \\ M^\pm_{he}(\alpha) & M^\pm_{hh}(\alpha) \end{bmatrix} \tag{14}$$

where

$$M^\pm_{ee}(\alpha) = \sin\alpha \pm \frac{1}{\eta}\sin\beta, \tag{15}$$

$$M^\pm_{eh}(\alpha) = -M^\pm_{he}(\alpha) = -\cos\alpha\cos\beta, \tag{16}$$

$$M_{hh}^{\pm}(\alpha) = \sin\alpha \pm \eta \sin\beta. \tag{17}$$

3. Solution

[8] The procedure is the same as that in *Osipov and Senior* [2008] and we give only the key steps. We start by writing

$$S_{e,h}(\alpha) = \Psi_{e,h}(\alpha)\Lambda_{e,h}(\alpha) \tag{18}$$

where $\Psi_{e,h}(\alpha)$ are auxiliary functions that satisfy

$$\begin{aligned}\left(\sin\alpha \pm \sin\theta_{e,h}\right)\Psi_{e,h}\left(\alpha \pm \frac{3}{4}\pi\right) = \\ \left(-\sin\alpha \pm \sin\theta_{e,h}\right)\Psi_{e,h}\left(-\alpha \pm \frac{3}{4}\pi\right)\end{aligned} \tag{19}$$

with

$$\sin\theta_e = \frac{1}{\eta}\sin\beta, \quad \sin\theta_h = \eta\sin\beta. \tag{20}$$

Because of the uniqueness condition, the real parts of the terms on the right-hand sides of (20) are non-negative, which implies that $\theta_{e,h}$ can be chosen such that $0 < \mathrm{Re}\,\theta_{e,h} \le \pi/2$.

[9] The functions satisfying (19) can be expressed in terms of the Maliuzhinets function $\psi_{3\pi/4}(\alpha)$ and are

$$\begin{aligned}\Psi_{e,h}(\alpha) = \frac{64}{81}&\left[\cos\frac{\alpha}{3} + \cos\left(\frac{\theta_{e,h}}{3} - \frac{\pi}{4}\right)\right] \\ &\cdot \left[\cos\frac{\alpha}{3} + \sin\left(\frac{\theta_{e,h}}{3} - \frac{\pi}{4}\right)\right] \\ &\cdot \left[\cos\frac{\alpha}{3} + \cos\left(\frac{\theta_{e,h}}{3} - \frac{\pi}{12}\right)\right] \\ &\cdot \left[\cos\frac{\alpha}{3} - \sin\left(\frac{\theta_{e,h}}{3} - \frac{\pi}{12}\right)\right] \\ &\cdot \left[\cos\frac{\alpha}{3} + \cos\left(\frac{\theta_{e,h}}{3} + \frac{\pi}{12}\right)\right]^{-1} \\ &\cdot \left[\cos\frac{\alpha}{3} + \sin\left(\frac{\theta_{e,h}}{3} + \frac{\pi}{12}\right)\right]^{-1}.\end{aligned} \tag{21}$$

These are free of poles and zeros in the strip Π_0. If we also write

$$\Lambda_{e,h}(\alpha) = \Lambda_{e,h}^{(0)}(\alpha) + \tilde{\Lambda}_{e,h}(\alpha) \tag{22}$$

where

$$\Lambda_e^{(0)}(\alpha) = \frac{E_{0z}}{\Psi_e(\phi_0)}\sigma(\alpha,\phi_0), \tag{23}$$

$$\Lambda_h^{(0)}(\alpha) = \frac{Z_0 H_{0z}}{\Psi_h(\phi_0)}\sigma(\alpha,\phi_0) \tag{24}$$

with

$$\sigma(\alpha,\phi_0) = \frac{2}{3}\frac{\cos(2\phi_0/3)}{\sin(2\alpha/3) - \sin(2\phi_0/3)}, \tag{25}$$

the unknown functions $\tilde{\Lambda}_{e,h}(\alpha)$ must be free of poles in the strip Π_0 and satisfy

$$\tilde{\Lambda}_e\left(\alpha \pm \frac{3}{4}\pi\right) - \tilde{\Lambda}_e\left(-\alpha \pm \frac{3}{4}\pi\right) = q_e^{\pm}(\alpha) + \tilde{q}_e^{\pm}(\alpha) \tag{26}$$

$$\tilde{\Lambda}_h\left(\alpha \pm \frac{3}{4}\pi\right) - \tilde{\Lambda}_h\left(-\alpha \pm \frac{3}{4}\pi\right) = q_h^{\pm}(\alpha) + \tilde{q}_h^{\pm}(\alpha) \tag{27}$$

where

$$\begin{aligned}\tilde{q}_e^{\pm}(\alpha) = \kappa_e^{\pm}(\alpha)\tilde{\Lambda}_h&\left(\alpha \pm \frac{3}{4}\pi\right) \\ &- \kappa_e^{\pm}(-\alpha)\tilde{\Lambda}_h\left(-\alpha \pm \frac{3}{4}\pi\right)\end{aligned} \tag{28}$$

$$\begin{aligned}\tilde{q}_h^{\pm}(\alpha) = \kappa_h^{\pm}(\alpha)\tilde{\Lambda}_e&\left(\alpha \pm \frac{3}{4}\pi\right) \\ &- \kappa_h^{\pm}(-\alpha)\tilde{\Lambda}_e\left(-\alpha \pm \frac{3}{4}\pi\right)\end{aligned} \tag{29}$$

with

$$\kappa_e^{\pm}(\alpha) = -\frac{M_{eh}^{\pm}(\alpha)\Psi_h(\alpha \pm 3\pi/4)}{M_{ee}^{\pm}(\alpha)\Psi_e(\alpha \pm 3\pi/4)} \tag{30}$$

$$\kappa_h^{\pm}(\alpha) = -\frac{M_{he}^{\pm}(\alpha)\Psi_e(\alpha \pm 3\pi/4)}{M_{hh}^{\pm}(\alpha)\Psi_h(\alpha \pm 3\pi/4)}. \tag{31}$$

The expressions for $q_e^{\pm}(\alpha)$ and $q_h^{\pm}(\alpha)$ differ from (28) and (29) in having $\tilde{\Lambda}_{e,h}(\alpha)$ replaced by the known functions $\Lambda_{e,h}^{(0)}(\alpha)$, and therefore serve as source terms in the inhomogeneous equations (26) and (27). When $\beta = \pi/2$ the right-hand sides of (26) and (27) vanish and the equations have the trivial solutions $\tilde{\Lambda}_{e,h}(\alpha) = 0$. We then recover the Maliuzhinets solution $S_{e,h}(\alpha) = \Psi_{e,h}(\alpha)\Lambda_{e,h}^{(0)}(\alpha)$.

[10] On application of a Fourier transform, modified by mapping on to the imaginary axis of the complex α

plane, and then using the fact that $q^{\pm}_{e,h}(\alpha)$ and $\tilde{q}^{\pm}_{e,h}(\alpha)$ are odd functions of α, (26) and (27) become

$$\tilde{\Lambda}_{e,h}(\alpha) = \int_0^{i\infty} \Big\{ K_+(\alpha,\tau)\Big[q^+_{e,h}(\tau) + \tilde{q}^+_{e,h}(\tau)\Big] + K_-(\alpha,\tau)\Big[q^-_{e,h}(\tau) + \tilde{q}^-_{e,h}(\tau)\Big]\Big\} d\tau \tag{32}$$

where

$$K_\pm(\alpha,\tau) = -\frac{i}{3\pi}\frac{\sin(2\tau/3)}{\sin(2\alpha/3) \mp \cos(2\tau/3)}. \tag{33}$$

Then if

$$w(\alpha) = -i\tan\Big(\frac{\alpha}{3}\Big), \quad w_0(\tau) = w\Big(\tau + \frac{3\pi}{4}\Big), \tag{34}$$

we have

$$K_\pm(\alpha,\tau) = \pm\frac{\big(1+w_0^2\big)(1-w^2)}{6\pi w_0(w \mp w_0)\big(w \pm w_0^{-1}\big)}, \tag{35}$$

which can be written as

$$K_\pm(\alpha,\tau) = \big[1 - w^2(\alpha)\big]\sum_{m=0}^{\infty} K^\pm_m(\tau) w^m(\alpha) \tag{36}$$

with $K^+_m(\tau) = (-1)^{m+1}\ K^-_m(\tau)$ and

$$K^-_m(\tau) = \frac{1}{6\pi}\big[w_0^{m+1}(\tau) + (-1)^m w_0^{-m-1}(\tau)\big]. \tag{37}$$

Substituting (36) into (32) leads to the series representation of the solution as

$$\tilde{\Lambda}_{e,h}(\alpha) = \big[1 - w^2(\alpha)\big]\sum_{m=0}^{\infty} C^{e,h}_m w^m(\alpha), \tag{38}$$

and by equating coefficients of like powers of w, we obtain a coupled system of algebraic equations from which the coefficients $C^{e,h}_m$ can be found. This completes the solution. To achieve any desired accuracy it is sufficient to retain only a finite number of terms in (38), and for all of the data presented in Section 5, the accuracy is better than 0.001.

4. High Frequency Analysis

[11] Once the spectra are determined, the Sommerfeld integrals (7) and (8) give the exact solution to the problem in the entire region outside the wedge. In the high-frequency limit when $k\rho\sin\beta \gg 1$, the integrals can be evaluated asymptotically using the steepest descent method to give

$$\overline{F} = \overline{F}_{\rm go} + \overline{F}_{\rm sw} + \overline{F}_{\rm d} \tag{39}$$

where

$$\overline{F} = \begin{bmatrix} E_z \\ Z_0 H_z \end{bmatrix}. \tag{40}$$

The geometrical optics field $\overline{F}_{\rm go}$ consists of the incident plane wave and the waves specularly reflected off the upper and lower faces of the wedge and is

$$\begin{aligned}\overline{F}_{\rm go} = {} & u(\pi - |\phi - \phi_0|)\overline{F}_{\rm inc}(\overline{r}) \\ & + e^{ikz\cos\beta + ik\rho\sin\beta\sin(\phi+\phi_0)} u\Big(\pi - \Big|\phi + \phi_0 - \frac{3}{2}\pi\Big|\Big) \\ & \cdot \overline{\overline{R}}_+\Big(\frac{3}{4}\pi - \phi_0\Big)\cdot \overline{F}_{\rm inc}(\overline{0}) \\ & + e^{ikz\cos\beta - ik\rho\sin\beta\sin(\phi+\phi_0)} u\Big(\pi - \Big|\phi + \phi_0 + \frac{3}{2}\pi\Big|\Big) \\ & \cdot \overline{\overline{R}}_-\Big(\frac{3}{4}\pi + \phi_0\Big)\cdot \overline{F}_{\rm inc}(\overline{0})\end{aligned} \tag{41}$$

where

$$\overline{F}_{\rm inc}(\overline{r}) = e^{i\overline{k}\cdot\overline{r}}\begin{bmatrix} E_{0z} \\ Z_0 H_{0z}\end{bmatrix} \tag{42}$$

and $u(x) = 1$ if $x > 0$ and 0 otherwise. In (41)

$$\overline{\overline{R}}_\pm(\chi) = \begin{bmatrix} R_{ee}(\chi) & \pm R_{eh}(\chi) \\ \pm R_{he}(\chi) & R_{hh}(\chi)\end{bmatrix} \tag{43}$$

with

$$R_{ee}(\chi) = -1 + \frac{2\sin\chi}{L(\chi)}(\eta\sin\beta + \sin\chi) \tag{44}$$

$$R_{eh}(\chi) = -R_{he}(\chi) = \frac{2\sin\chi\cos\chi\cos\beta}{L(\chi)} \tag{45}$$

$$R_{hh}(\chi) = -1 + \frac{2\sin\chi}{L(\chi)}\Big(\frac{1}{\eta}\sin\beta + \sin\chi\Big) \tag{46}$$

and

$$\begin{aligned}L(\chi) &= \det\overline{\overline{M}}_\pm(\pm\chi) \\ &= (\eta + \sin\chi\sin\beta)\Big(\frac{1}{\eta} + \sin\chi\sin\beta\Big).\end{aligned} \tag{47}$$

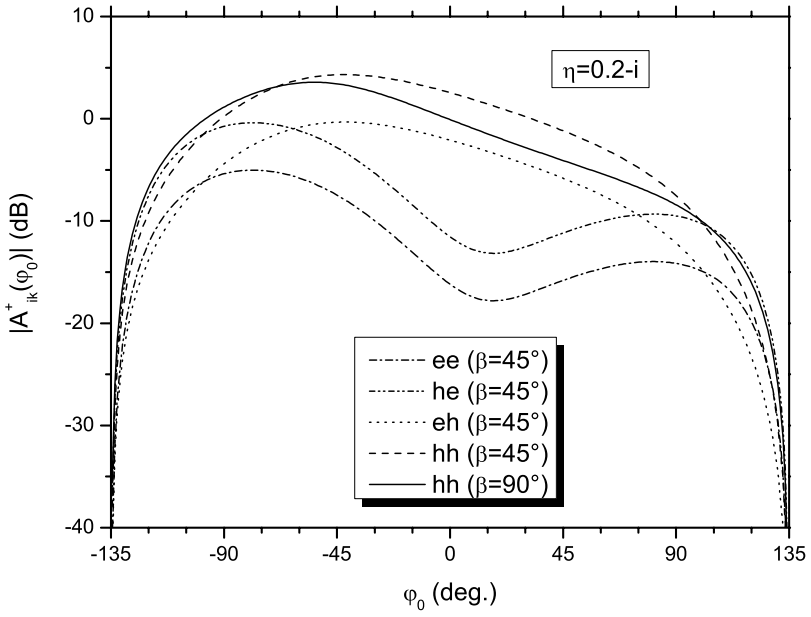

Figure 2. Components of the amplitude $\overline{A}_+$ of the surface wave on the upper face of a wedge with $\eta = 0.2 - i$ as a function of illumination aspect ϕ_0 for $\beta = \pi/2$ and $\pi/4$ and various polarization of the incident wave: first and second curves - $E_{0z} = 1$ and $H_{0z} = 0$; the rest curves - $E_{0z} = 0$ and $Z_0 H_{0z} = 1$.

[12] The surface wave field is made up of the surface waves supported by the upper and lower faces of the wedge and is

$$\overline{F}_{\rm sw} = \overline{F}_+ + \overline{F}_- \tag{48}$$

where

$$\overline{F}_\pm = \overline{A}_\pm e^{ikz\cos\beta - ik\rho\sin\beta\cos(\tilde{\chi}\mp\phi+3\pi/4)} \tag{49}$$

if $\alpha_\pm \in \Pi_{\rm sdp}$, and $\overline{F}_\pm = \overline{0}$ otherwise. In (49) $\alpha_\pm = -\phi \pm (3\pi/4 + \tilde{\chi})$, $\Pi_{\rm sdp}$ is the region of the complex α plane between the steepest descent paths through $\alpha = \pm\pi$,

$$\tilde{\chi} = \begin{cases} \pi + \arcsin(\eta/\sin\beta) & \text{if } \mathrm{Im}\,\eta < 0 \\ \pi + \arcsin(1/(\eta\sin\beta)) & \text{if } \mathrm{Im}\,\eta > 0 \end{cases} \tag{50}$$

$$\overline{A}_\pm = \mp\frac{1}{L'(\tilde{\chi})} L(\tilde{\chi})\overline{\overline{R}}_\pm(\tilde{\chi})\cdot\overline{S}\left(\pm\frac{3}{4}\pi \mp \tilde{\chi}\right) \tag{51}$$

and the prime denotes the derivative.

[13] The third term of (39) is the edge-diffracted field

$$\overline{F}_{\rm d} = \frac{e^{ikz\cos\beta + ik\rho\sin\beta + i\pi/4}}{\sqrt{2\pi k\rho\sin\beta}} \cdot \left[\overline{S}(\phi-\pi) - \overline{S}(\phi+\pi)\right]. \tag{52}$$

In a ray-fixed coordinate system (Figure 1) the diffracted field

$$\overline{E}_{\rm d} = \begin{bmatrix} E^{\rm d}_\beta \\ E^{\rm d}_\phi \end{bmatrix} \tag{53}$$

and the incident field

$$\overline{E}_{\rm inc} = \begin{bmatrix} E^{\rm inc}_{\beta_{\rm inc}} \\ E^{\rm inc}_{\phi_{\rm inc}} \end{bmatrix} \tag{54}$$

are related by the formula

$$\overline{E}_{\rm d}(\overline{r}) = \frac{e^{ikr}}{\sqrt{r}}\overline{\overline{D}}\cdot\overline{E}_{\rm inc}(\overline{0}) \tag{55}$$

where the diffraction coefficient is the tensor

$$\overline{\overline{D}} = \frac{e^{i\pi/4}}{\sin\beta\sqrt{2\pi k}}\begin{bmatrix} -D_{ee} & D_{eh} \\ D_{he} & -D_{hh} \end{bmatrix} \tag{56}$$

whose elements are expressed in terms of the spectra as

$$\begin{aligned} D_{ee} &= S_e(\phi-\pi) - S_e(\phi+\pi) \\ D_{he} &= S_h(\phi-\pi) - S_h(\phi+\pi) \end{aligned} \tag{57}$$

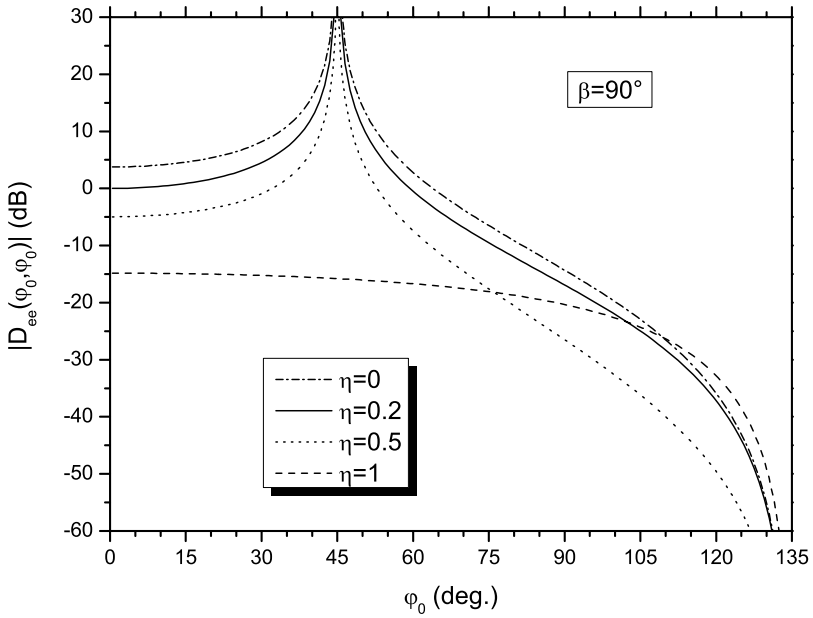

Figure 3. Monostatic, ee case, $\beta = \pi/2$.

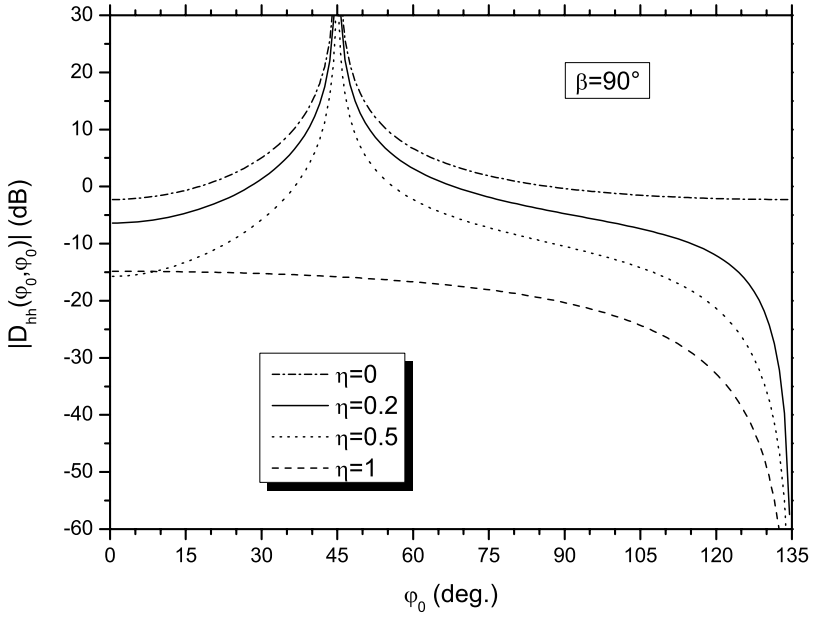

Figure 4. Monostatic, hh case, $\beta = \pi/2$.

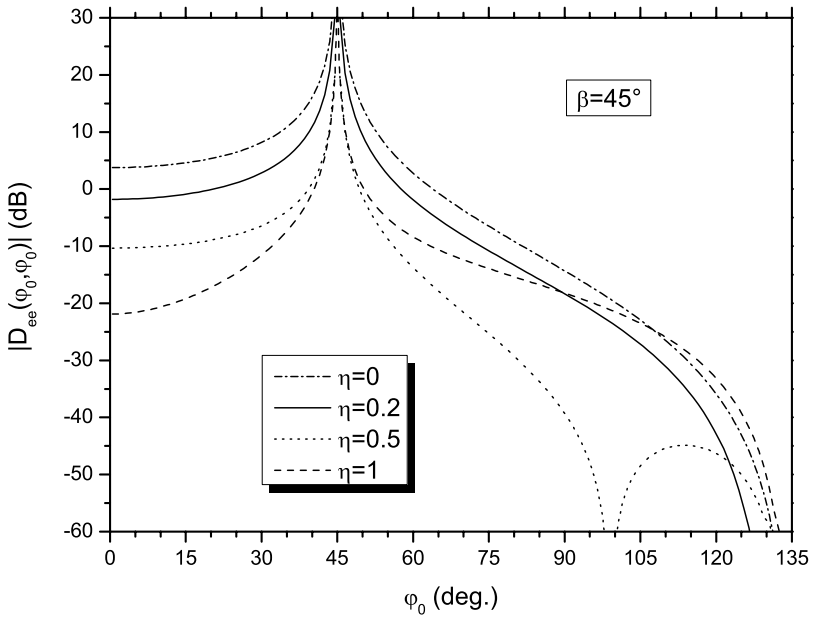

Figure 5. Monostatic, ee case, $\beta = \pi/4$.

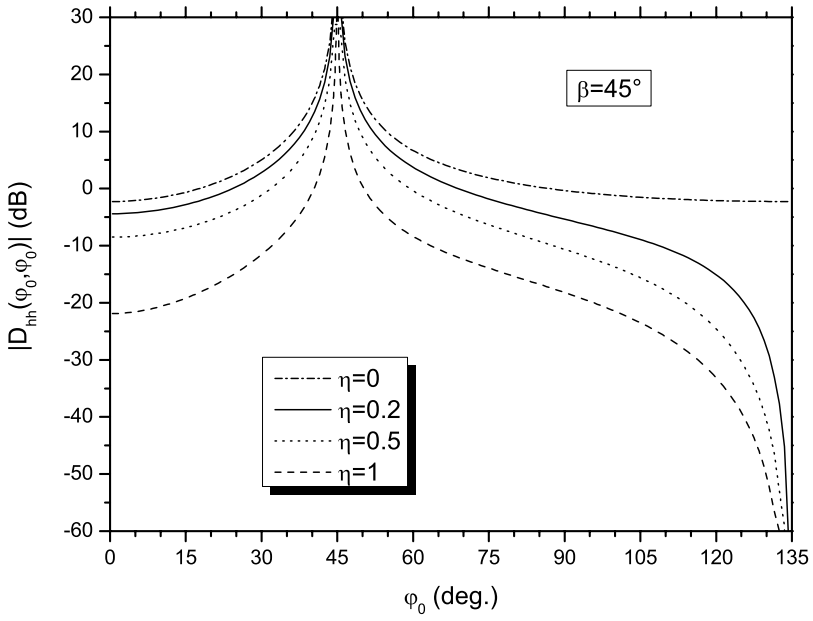

Figure 6. Monostatic, hh case, $\beta = \pi/4$.

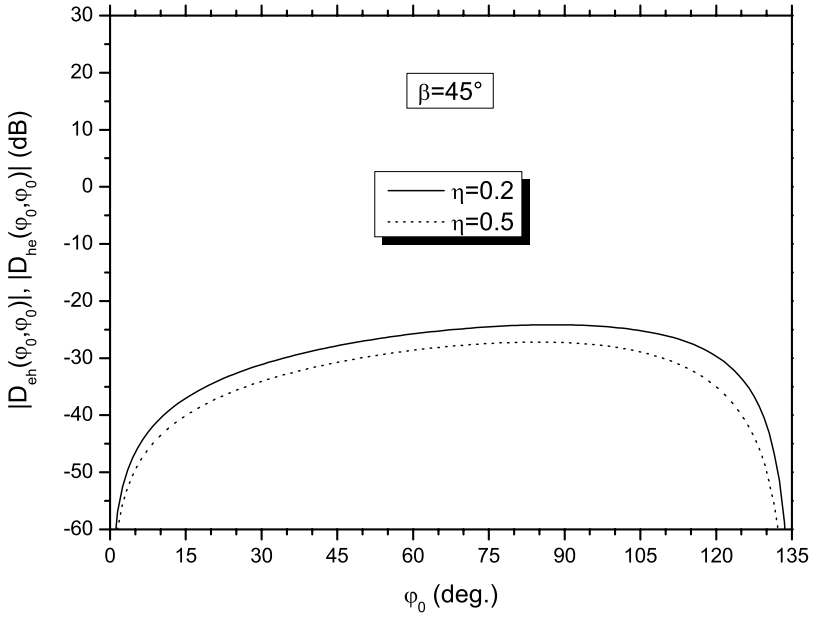

Figure 7. Monostatic, eh and he cases, $\beta = \pi/4$.

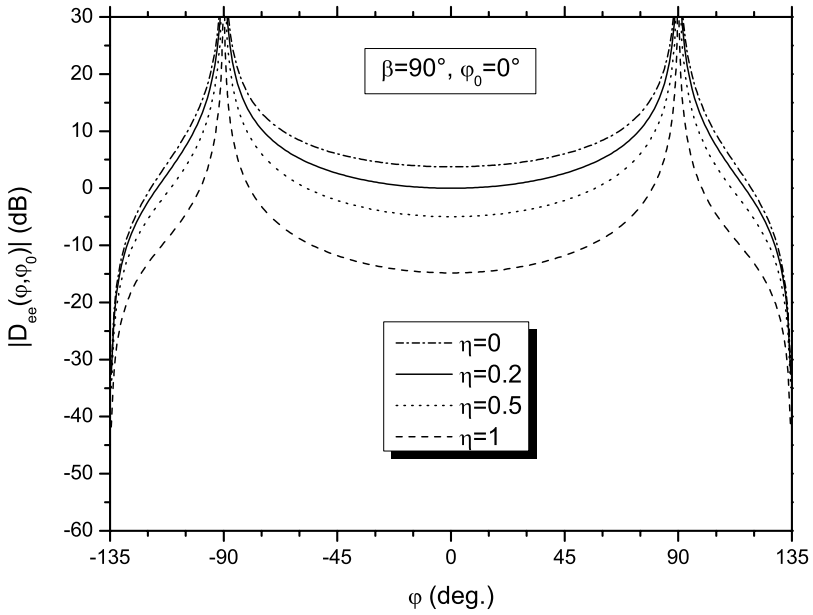

Figure 8. Bistatic, ee case, $\beta = \pi/2$, $\phi_0 = 0$.

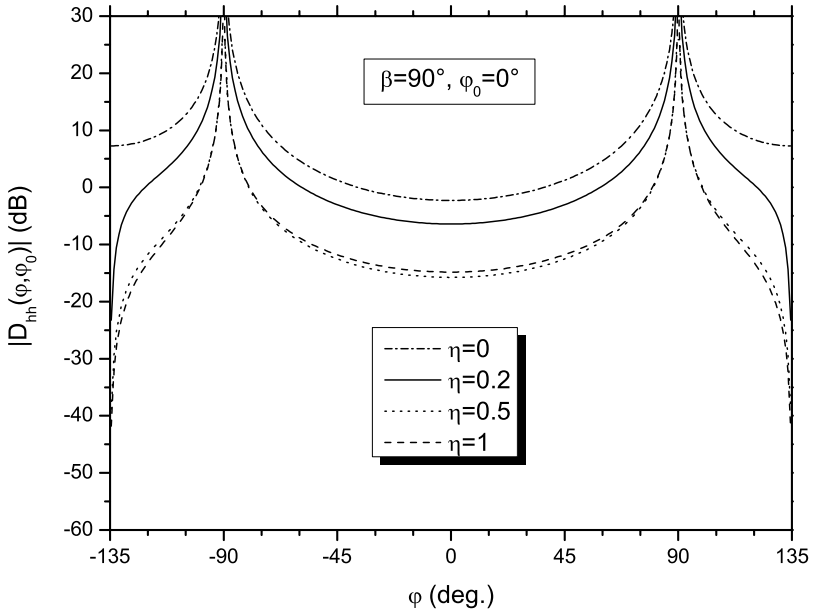

Figure 9. Bistatic, hh case, $\beta = \pi/2$, $\phi_0 = 0$.

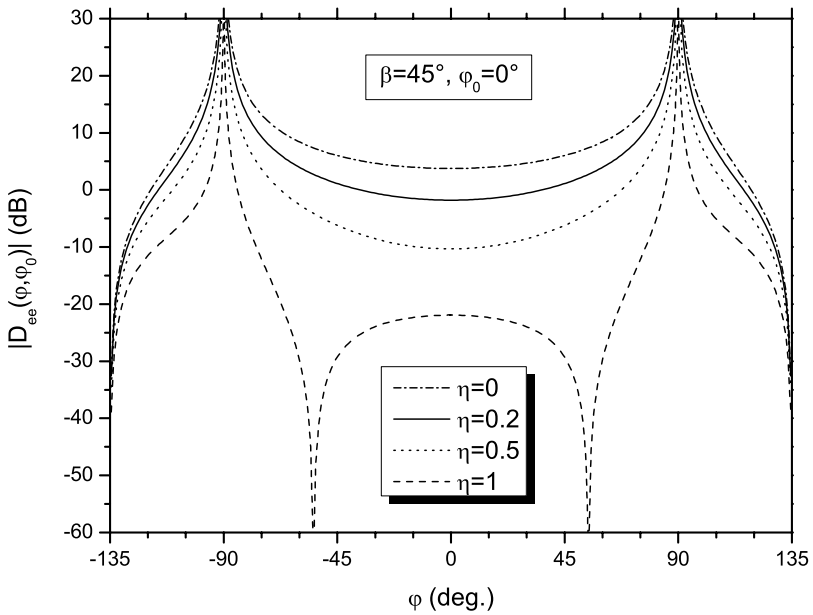

Figure 10. Bistatic, ee case, $\beta = \pi/4$, $\phi_0 = 0$.

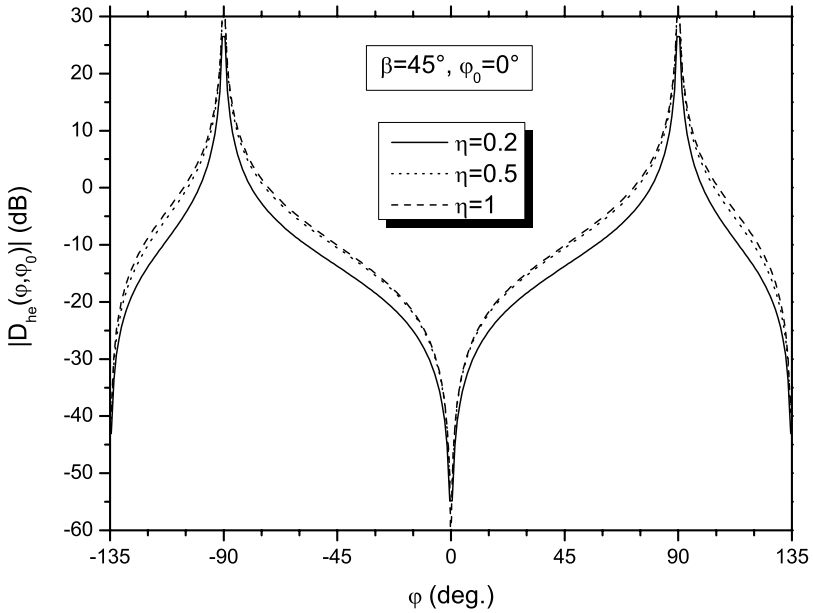

Figure 11. Bistatic, he case, $\beta = \pi/4$, $\phi_0 = 0$.

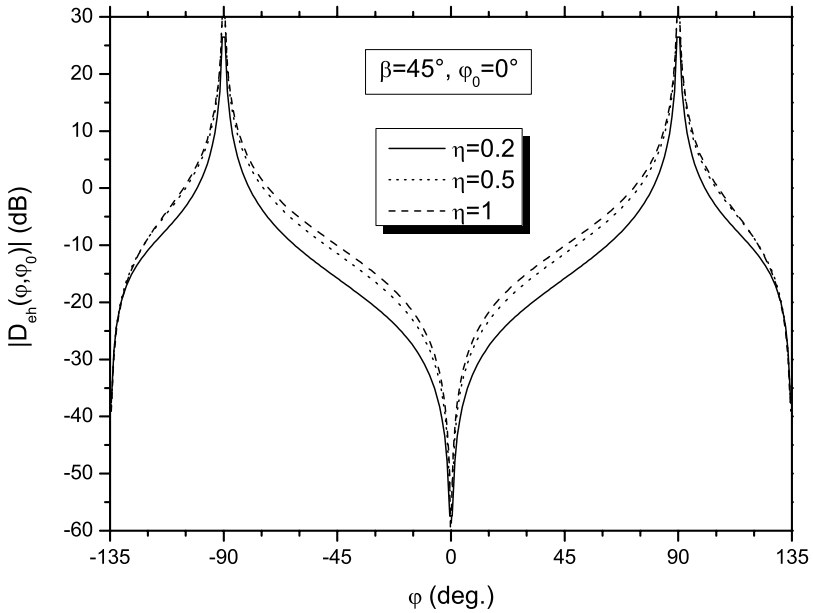

Figure 12. Bistatic, eh case, $\beta = \pi/4$, $\phi_0 = 0$.

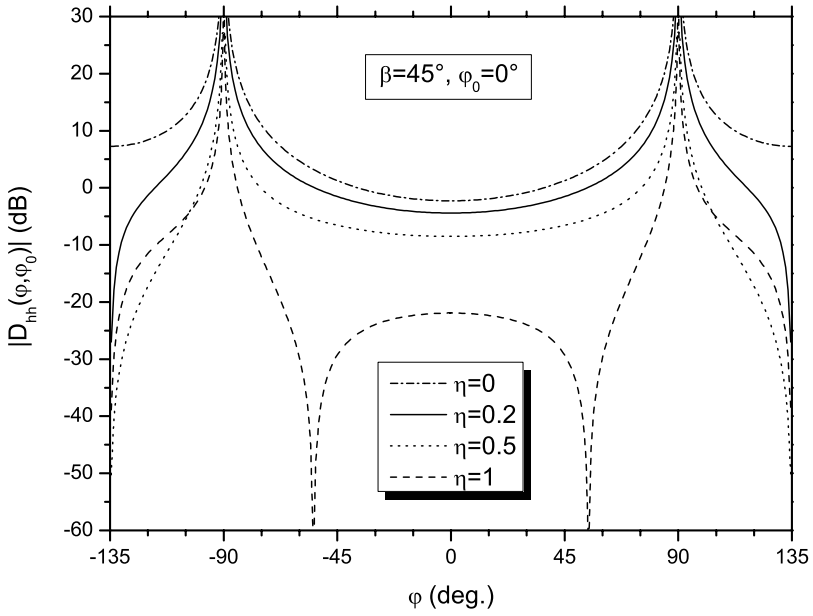

Figure 13. Bistatic, hh case, $\beta = \pi/4$, $\phi_0 = 0$.

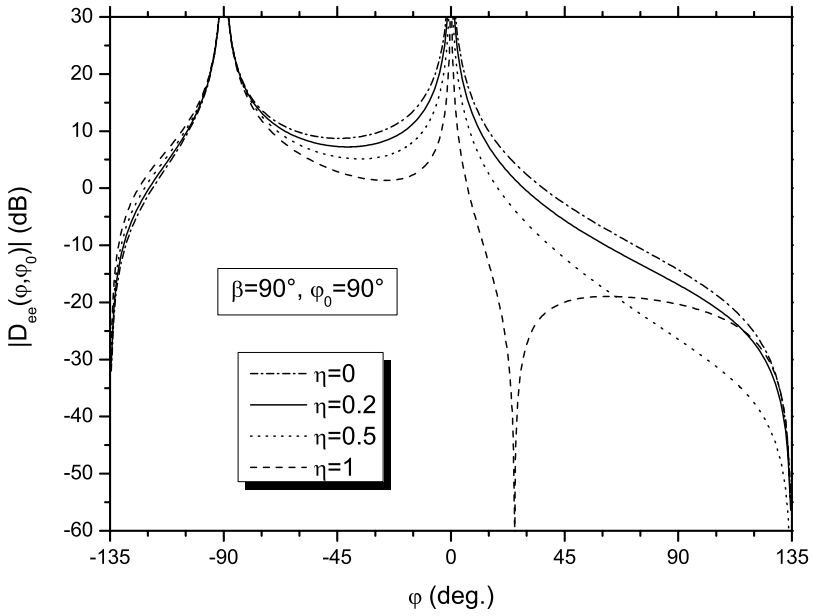

Figure 14. Bistatic, ee case, $\beta = \pi/2$, $\phi_0 = \pi/2$.

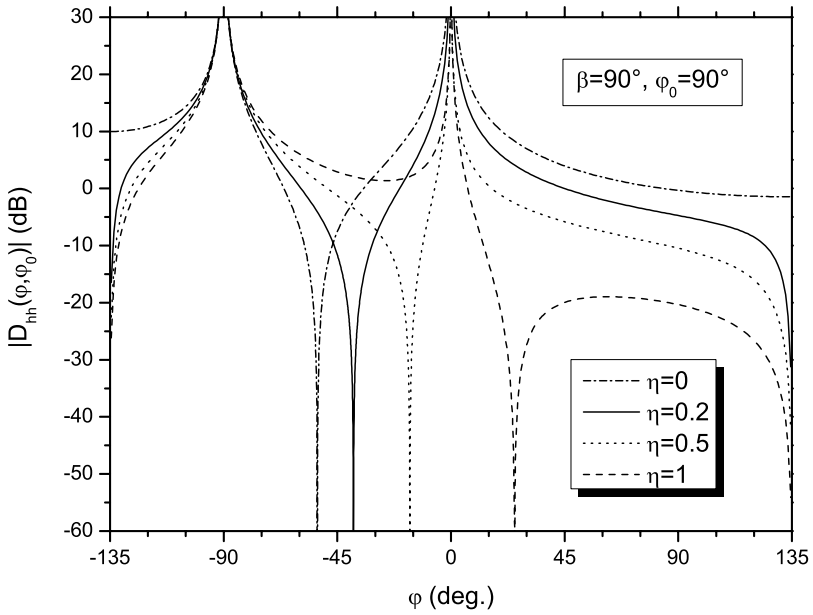

Figure 15. Bistatic, hh case, $\beta = \pi/2$, $\phi_0 = \pi/2$.

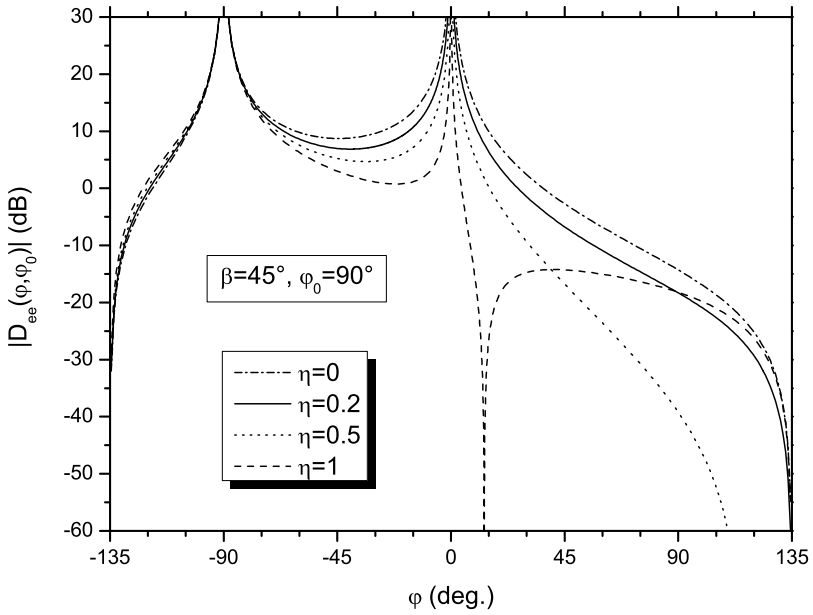

Figure 16. Bistatic, ee case, $\beta = \pi/4$, $\phi_0 = \pi/2$.

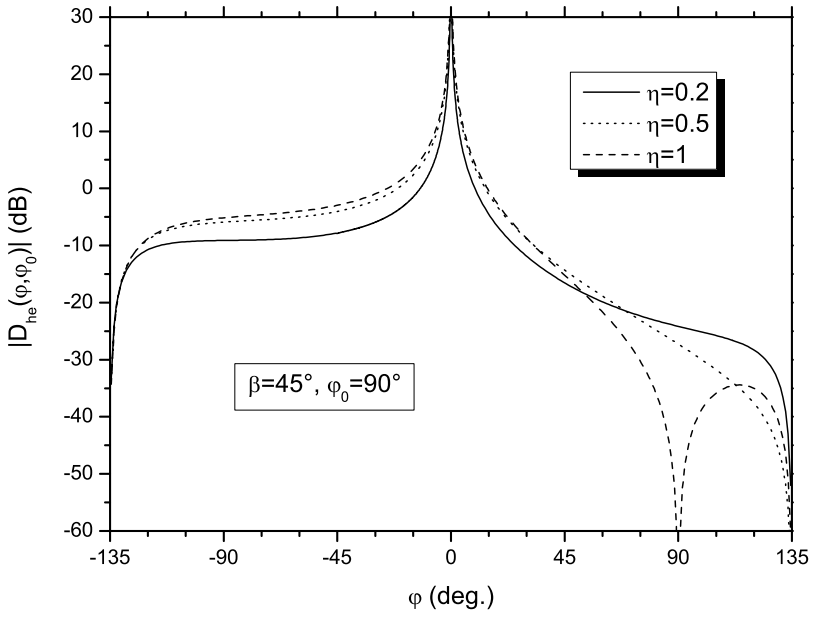

Figure 17. Bistatic, he case, $\beta = \pi/4$, $\phi_0 = \pi/2$.

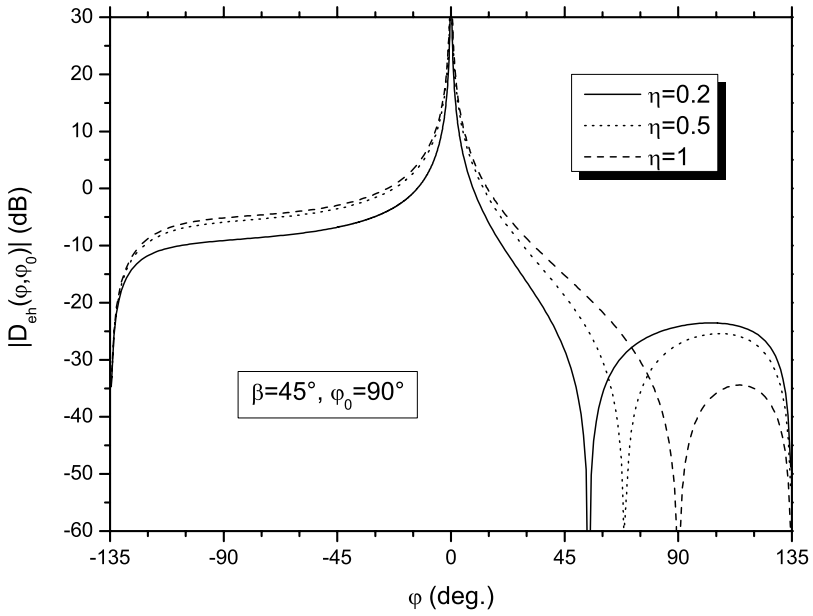

Figure 18. Bistatic, eh case, $\beta = \pi/4$, $\phi_0 = \pi/2$.

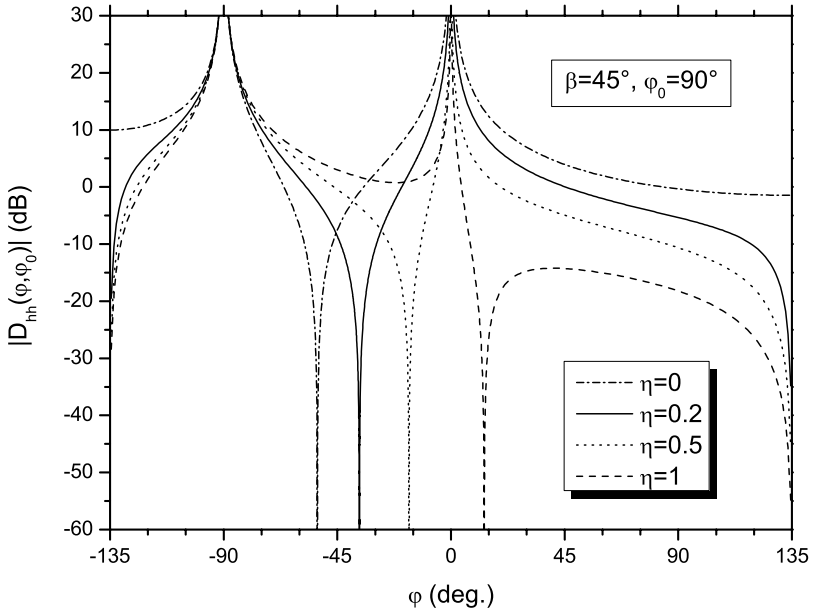

Figure 19. Bistatic, hh case, $\beta = \pi/4$, $\phi_0 = \pi/2$.

where $E_{0z} = 1$ and $H_{0z} = 0$, and

$$D_{eh} = S_e(\phi - \pi) - S_e(\phi + \pi)$$
$$D_{hh} = S_h(\phi - \pi) - S_h(\phi + \pi) \tag{58}$$

where $E_{0z} = 0$ and $H_{0z} = 1/Z_0$. It can be shown that

$$\begin{aligned} D_{ee}(\phi, \phi_0, \beta) &= D_{ee}(\phi_0, \phi, \beta) \\ &= D_{ee}(\phi, \phi_0, \pi - \beta) \\ D_{eh}(\phi, \phi_0, \beta) &= D_{he}(\phi_0, \phi, \beta) \\ &= -D_{eh}(\phi, \phi_0, \pi - \beta) \\ D_{he}(\phi, \phi_0, \beta) &= D_{eh}(\phi_0, \phi, \beta) \\ &= -D_{he}(\phi, \phi_0, \pi - \beta) \\ D_{hh}(\phi, \phi_0, \beta) &= D_{hh}(\phi_0, \phi, \beta) \\ &= D_{hh}(\phi, \phi_0, \pi - \beta), \end{aligned} \tag{59}$$

and from the boundary conditions (5) and (6) it follows that

$$\begin{aligned} D_{ee}(\phi, \phi_0, \beta, \eta^{-1}) &= D_{hh}(\phi, \phi_0, \beta, \eta) \\ D_{eh}(\phi, \phi_0, \beta, \eta^{-1}) &= -D_{he}(\phi, \phi_0, \beta, \eta) \\ D_{he}(\phi, \phi_0, \beta, \eta^{-1}) &= -D_{eh}(\phi, \phi_0, \beta, \eta) \\ D_{hh}(\phi, \phi_0, \beta, \eta^{-1}) &= D_{ee}(\phi, \phi_0, \beta, \eta) \end{aligned} \tag{60}$$

Equations (60) imply that it is sufficient to study impedances with $|\eta| \leq 1$.

5. Numerical Results

[14] Figure 2 shows the amplitude $\overline{A}_+$ of the surface wave excited on the upper face of a wedge with $\eta = 0.2 - i$ as a function of the incidence angle ϕ_0 for $\beta = \pi/2$ and $\pi/4$. We write $\overline{A}_+ = [A^+_{ee}, A^+_{he}]'$ when $E_{0z} = 1$, $H_{0z} = 0$ and $\overline{A}_+ = [A^+_{eh}, A^+_{hh}]'$ when $E_{0z} = 0$, $Z_0 H_{0z} = 1$, where the dash denotes the transposition. Since Im $\eta < 0$, (50) gives $\tilde{\chi} = \pi + \arcsin(\eta/\sin\beta)$, and A^+_{hh} is the only component that does not vanish in the case of normal incidence (solid line). For $\beta = \pi/4$ all components of the surface wave get excited. The curves for A^+_{ee} and A^+_{he} as well as A^+_{eh} and A^+_{hh} differ from each other by a factor (a shift in dB scale) which depends on η and β but is independent of ϕ_0, resulting from the relations

$$\frac{A^+_{ee}}{A^+_{he}} = \frac{A^+_{eh}}{A^+_{hh}} = \frac{R_{he}(-\tilde{\chi})}{R_{ee}(-\tilde{\chi})} = \frac{R_{hh}(-\tilde{\chi})}{R_{eh}(-\tilde{\chi})} \tag{61}$$

satisfied by the z components of the electric and magnetic fields in the surface wave.

[15] The diffracted field components are functions of ϕ, ϕ_0, β and η, and to illustrate their behavior, results are

presented for a variety of these quantities. The values chosen for η are 0, 0.2, 0.5 and 1, and in view of (60), the results also apply for $\eta = 2$, 5 and ∞. These cover the range of values encountered in many wireless applications, and the imaginary part of η is neglected since it is normally quite small. When $\eta = 1$ the geometry is polarization-independent, implying (see (60)) that $D_{hh} = D_{ee}$ and $D_{he} = -D_{eh}$, and when $\phi_0 = \phi$, $D_{he} = D_{eh} = 0$ for all ϕ and β. The latter are also zero when $\beta = \pi/2$ for all ϕ, ϕ_0 and η or when $\eta = 0$ (or ∞) for all ϕ, ϕ_0 and β.

[16] The monostatic (or backscattered) field is plotted as a function of $\phi = \phi_0$, $0 \leq \phi_0 < 3\pi/4$, for $\beta = \pi/2$ in Figures 3 and 4 and for $\beta = \pi/4$ in Figures 5–7. The infinity at $\phi_0 = \pi/4$ is necessary to account for the specularly reflected field except for $\eta = 1$ and $\beta = \pi/2$ when the reflection coefficient is zero.

[17] For axial incidence ($\phi_0 = 0$) the bistatic field is plotted as a function of ϕ, $-3\pi/4 < \phi < 3\pi/4$, for $\beta = \pi/2$ in Figures 8 and 9, and for $\beta = \pi/4$ in Figures 10–13. The polarization dependence is relatively little, and the general shape of the curves for D_{ee} and D_{hh} is similar. This is also true for D_{he} and D_{eh}. The analogous results for $\phi_0 = \pi/2$ are shown in Figures 14–19. For this angle of incidence the dependence on β is relatively small, and the curves in Figures 14 and 16 are similar, as are those in Figures 15 and 19, and Figures 17 and 18.

References

Bernard, J.-M. L. (1998), Diffraction at skew incidence by an anisotropic impedance wedge in electromagnetism theory: a new class of canonical cases, *J. Phys. A: Math. Gen.*, *31*, 595–613.

Budaev, B. V., and D. B. Bogy (2006), Diffraction of a plane skew electromagnetic wave by a wedge with general anisotropic impedance boundary conditions, *IEEE Trans. Antennas Propag.*, *54*, 1559–1567.

Daniele, V. G., and G. Lombardi (2006), Wiener-Hopf solution for impenetrable wedges at skew incidence, *IEEE Trans. Antennas Propag.*, *54*, 2472–2485.

Lyalinov, M. A., and N. Y. Zhu (2006), Diffraction of a skew incident plane electromagnetic wave by an impedance wedge, *Wave Motion*, *44*, 21–43.

Maliuzhinets, G. D. (1958), Excitation, reflection and emission of surface waves from a wedge with given face impedances, *Sov. Phys. Dokl.*, *3*, 752–755.

Osipov, A. V., and T. B. A. Senior (2008), Electromagnetic diffraction by arbitrary-angle impedance wedges, *Proc. R. Soc. A*, *464*, 177–195, doi:10.1098/rspa.2007.0163.

Pelosi, G., G. Manara, and P. Nepa (1998), A UTD solution for the scattering by a wedge with anisotropic impedance faces: skew incidence case, *IEEE Trans. Antennas Propag.*, *46*, 579–588.

Rojas, R. G. (1988), Electromagnetic diffraction of an obliquely incident plane wave field by a wedge with impedance faces, *IEEE Trans. Antennas Propag.*, *36*, 956–970.

Senior, T. B. A., and J. L. Volakis (1986), Scattering by an imperfect right-angled wedge, *IEEE Trans. Antennas Propag.*, *34*, 681–689.

Syed, H. H., and J. L. Volakis (1992), An approximate skew incidence diffraction coefficient for an impedance wedge, *Electromagnetics*, *12*, 33–55.

Vaccaro, V. G. (1981), Electromagnetic diffraction from a right-angled wedge with soft conditions on one face, *Opt. Acta*, *28*, 293–311.

A. V. Osipov, Microwaves and Radar Institute, German Aerospace Center, DLR, 82234 Wessling, Germany. (andrey.osipov@dlr.de)

T. B. A. Senior, Department of Electrical Engineering and Computer Science, University of Michigan, Ann Arbor, MI 48109-2122, USA. (senior@eecs.umich.edu)